Magnetization scissoring in aluminum/Permalloy microstructures

L. Yuan,[1] D. S. Wisbey,[1] S. T. Halloran,[1] D. P. Pappas,[1] F. C. S. da Silva,[2] and H. Z. Fardi[2,a)]
[1]*National Institute of Standards and Technology, Boulder, Colorado 80305, USA*
[2]*Department of Electrical Engineering, University of Colorado Denver, Denver, Colorado 80217-3364, USA*

(Received 7 July 2009; accepted 24 October 2009; published online 10 December 2009)

Induced scissoring of magnetization has been observed in aluminum/Permalloy ($Ni_{81}Fe_{19}$) thin films upon application of an alternating current. Harmonic analysis of the magnetoresistance indicates that the magnetization in the top and bottom portions of the film can rotate $\pm 20°$ from the axis along which the current is applied. The opposite angles of rotation, or scissoring, can be explained by internal oersted fields from the current. These oersted fields will rotate the in-plane magnetization of the film in opposite directions through the thickness of the film. Simulation using OOMMF shows a high degree of correlation with the observed data. © *2009 American Institute of Physics*.
[doi:10.1063/1.3264664]

I. INTRODUCTION

A homogeneous current passing through a conducting microstructure will generate a nonuniform internal oersted magnetic field.[1] The magnetization through the film will be affected by these oersted fields and will tend to rotate in opposite directions or scissor relative to each other. Figure 1 shows how the magnetization can rotate in opposite directions on opposite sides of a coupling stripe. Prior research has addressed the magnetization reversal process with an applied external field, such as magnetic coherent rotation,[2] magnetic curling,[3–5] and magnetic fanning.[6,1] Other studies have focused on current-driven domain wall motion.[7–13] Early studies of this effect were conducted on samples with large dimensions, on the order of hundreds of micrometers.[1] However, recent work has shown that these internal Oersted fields are critical in the switching of structures with submicron meter dimensions.[5,12,14,15] Methods used to study the magnetization behavior include magnetic force microscopy, superconducting quantum interference devices, magneto-optic Kerr effect, and Lorentz microscopy. These methods measure either the average volume magnetization of the sample or surface magnetization. Due to the shrinking feature size, understanding the role of bias field and magnetization in samples with feature size comparable to the domain size[16] are important.

In this paper, we investigate the magnetization behavior induced by a current in thin film Permalloy ($Ni_{81}Fe_{19}$) samples with widths ranging from 0.2 to 1 μm, using the second and third harmonic magnetoresistance (MR) measurements. We show that the magnetization scissoring between the top and the bottom surfaces of the film is induced by an internal oersted magnetic field.

We fabricated three types of different layer structures as shown in Fig. 2: an aluminum layer under the Permalloy layer, an aluminum layer between two Permalloy layers, and a single layer of Permalloy. The rotation in the magnetization in a single thin film of Permalloy is modeled by analyzing the second and third harmonics of the MR in the aluminum/Permalloy samples. Separating the current path from the magnetization allows us to more clearly see the rotation caused by the oersted fields. We found a scissoring behavior for these samples and we calculated the scissoring angle using an analytical model. The scissoring angle extracted from the experimental data matches with the simulation results obtained using NIST's object oriented magnetic modeling framework, OOMMF,[17] simulation tool. Our measurements indicate magnetic scissoring angles of up to 20° with respect to the long axis of the conductor with a current density of 2×10^8 A/cm^2. We also show that the amplitude of the magnetic scissoring depends on the current density and as well as the width to thickness ratio of the single-layer Permalloy conductor.

II. EXPERIMENT

The three types of samples were fabricated by electron-beam lithography using a lift-off process. The films were deposited by electron-beam evaporation. We evaluated three types of conductors (thickness shown in nanometers):

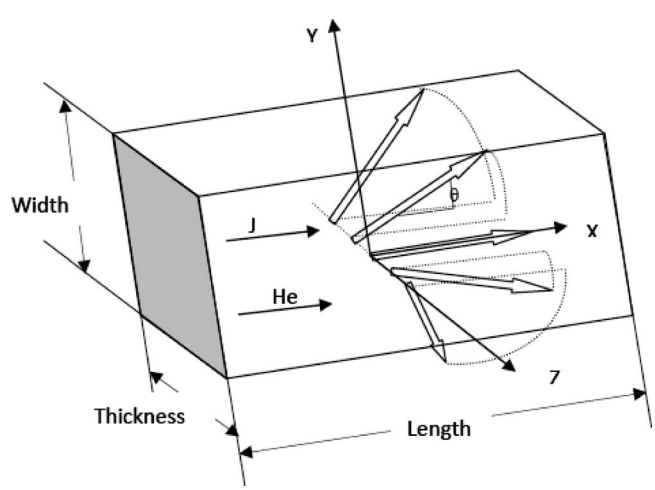

FIG. 1. Magnetization scissoring in a thin magnetic stripe (Ref. 1).

a)Electronic mail: hamid.fardi@ucdenver.edu.

 © 2009 American Institute of Physics

Downloaded 03 Feb 2010 to 132.163.130.151. Redistribution subject to AIP license or copyright; see http://jap.aip.org/jap/copyright.jsp

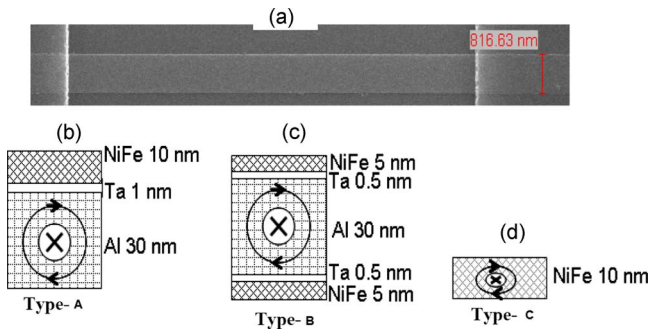

FIG. 2. (Color online) (a) SEM picture of one bar and the layer structures of (b) type A, (c) type B, and (d) type C samples. The direction of the oersted field inside the sample is shown.

(1) Type A: bilayer Al30/Ta1/$Ni_{81}Fe_{19}$10;
(2) Type B: trilayer $Ni_{81}Fe_{19}$5/Ta0.5/Al30/Ta0.5/$Ni_{81}Fe_{19}$5;
(3) Type C: single layer $Ni_{81}Fe_{19}$10, $Ni_{81}Fe_{19}$30 and $Ni_{81}Fe_{19}$50.

For each type of layer structure, the samples widths were varied from 0.2 to 1 μm where the lengths and the thicknesses were kept fixed at 10 and 0.8 μm, respectively. Samples with the same layer structure but different widths were deposited at the same time. The room temperature harmonic measurements were performed with a lock-in technique. A Wheatstone bridge method was used to remove the large primary or dc term in order to obtain high resolution data at higher order harmonic measurements. The samples were biased with an ac current at 1 kHz.

III. RESULTS AND DISCUSSION

Figure 3 compares the second and third harmonic measurements of the three sample types after removing field-independent effects such as thermal and other nonlinear measurement artifacts. The total current in $Ni_{81}Fe_{19}$ layers was kept nominally constant in all samples to obtain a direct comparison. This was achieved by calculating the parallel resistance of the layers based on bulk resistivity, adjusting the current to 400 μA in the $Ni_{81}Fe_{19}$ layers and keeping the applied magnetic field (H) perpendicular to the direction of applied current.

Results from type A samples, Al/$Ni_{81}Fe_{19}$ bilayer, show that the second harmonic amplitude is an odd function of the applied magnetic field and that there is no evidence of a field-dependent third harmonic signal [inset of Fig. 3(a)]. In this structure, most of the current passes through the aluminum layer due to its lower resistance. This current generates an oersted field in Permalloy layer. Therefore, the magnetization of the Permalloy layer will rotate with total field, which includes both an external applied field (H_e) and the oersted magnetic field induced by the bias current.

Using a simplified model,[11] assuming that the magnetization of the $Ni_{81}Fe_{19}$ layer rotates coherently with the applied field due to the elongated shape of the microstructure, the rotation angle (θ) measured with respect to the direction of applied current can then be written as

$$\sin\theta = \frac{H_e + SI}{H_k} \quad \text{for} \quad H_e + SI < H_k, \tag{1}$$

where S is the coefficient representing the effect of the induced oersted magnetic field and the applied current, I. H_k is the anisotropy field of the structure. The rotating angle θ and the coefficient S are the average values over the volume of the sample. The voltage output V is then written as

$$V = I \times R_{\text{total}}, \tag{2}$$

where R_{total} is the total resistance of the sample

$$R_{\text{total}} = \frac{1}{\dfrac{1}{R_{Ni_{81}Fe_{19}}} + \dfrac{1}{R_{\text{Al}}}}. \tag{3}$$

In Eq. (3) R_{Al} is the resistance of the aluminum layer and $R_{Ni_{81}Fe_{19}}$ is the resistance of Permalloy layer defined as

$$R_{Ni_{81}Fe_{19}} = R_0 + \Delta R \cos^2\theta = R_0 + \Delta R\left[1 - \left(\frac{H_e + SI}{H_k}\right)^2\right]. \tag{4}$$

In Eq. (4), R_0 is the resistance when the rotation angle θ equals to 90° and ΔR is the difference in the resistance values when θ=90° and θ=0°. Since the thermal term only gives a field-independent dc bias, it is not included in the above derivation.

The simulated second and third harmonic terms are computed by a Fourier transform of the voltage calculated from Eq. (1). From the anisotropic MR measurement at an applied bias current of 10 μA, the values of R_0=479 Ω, ΔR =5.98 Ω, and H_k=8623 A/m are obtained. These experimental data are then fitted to a single parameter S =7.0 m^{-1} shown by the solid line in Figs. 3(a) and 3(b).

Results from type B samples, $Ni_{81}Fe_{19}$/Al/$Ni_{81}Fe_{19}$ trilayer, show the appearance of a third harmonic signal as shown in Figs. 3(c) and 3(d). As derived below, this signal indicates scissoring which is a parabolic function of the applied magnetic field. Here, the oersted field induced by the applied bias current has an opposite direction at the top and the bottom Permalloy layers [inset of Fig. 3(c)]. Therefore, the magnetizations of the top and the bottom Permalloy layers rotate in opposite directions following the oersted field.

In magnetic scissoring regime, the resistance of the aluminum layer is in parallel with the resistance of the Permalloy layers. From Eq. (2) the total resistance is given by

$$\frac{1}{R_{\text{total}}} = \frac{1}{R_t} + \frac{1}{R_b} + \frac{1}{R_{\text{Al}}}, \tag{5}$$

where R_t is the resistance of the top Permalloy layer

$$R_t = R_0 + \Delta R \cos^2\theta_t \approx R_0 + \Delta R\left[1 - \left(\frac{+SI + H_e}{H_k}\right)^2\right], \tag{6}$$

and R_b is the resistance of the bottom Permalloy layer

Downloaded 03 Feb 2010 to 132.163.130.151. Redistribution subject to AIP license or copyright; see http://jap.aip.org/jap/copyright.jsp

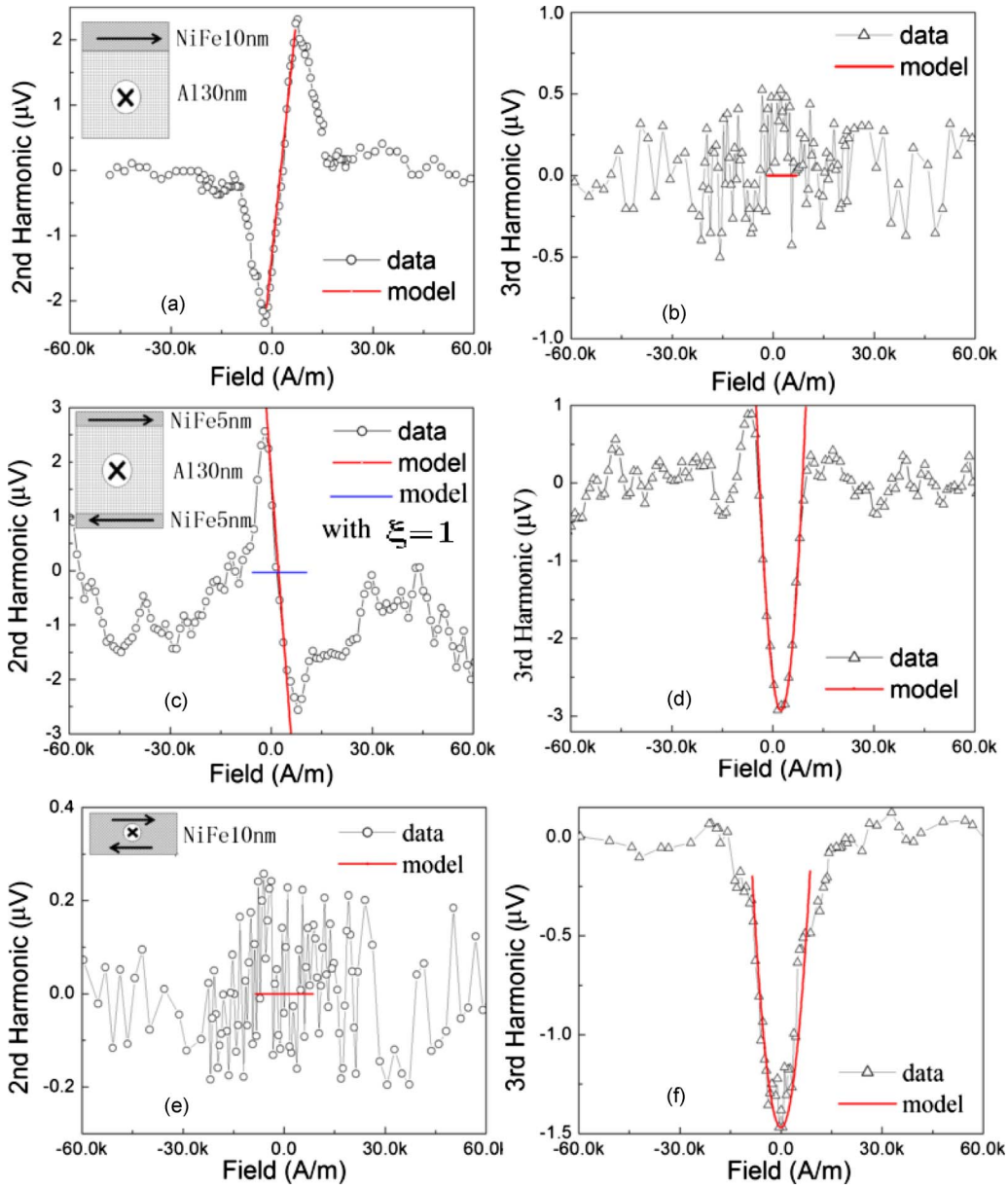

FIG. 3. (Color online) The second and third harmonic measurements (open point) and model (solid line) after removing field-independent effects such as thermal and other nonlinear measurement artifacts for samples [(a) and (b)] type A Al30/Ta1/$Ni_{81}Fe_{19}$10, [(c) and (d)] type B $Ni_{81}Fe_{19}$5/Ta0.5/Al30/Ta0.5/$Ni_{81}Fe_{19}$5, and [(e) and (f)] type C $Ni_{81}Fe_{19}$10 (thicknesses in nanometer). The dimension of the sample is $0.8\times 10\ \mu m^2$. The insets show the direction of the induced oersted field inside the $Ni_{81}Fe_{19}$ layer.

$$R_b = R_0 + \Delta R \cos^2 \theta_b \approx R_0 + \Delta R\left[1 - \left(\frac{-\xi SI + H_e}{H_k}\right)^2\right]. \tag{7}$$

The parameter ξ is a modeling parameter included to take into account any slight asymmetry in the oersted magnetic field and its effect on the top and bottom layers.

From comparison between the Fourier transform of the output voltage obtained from Eqs. (1)–(7) and the experimental data of the second and third harmonic signals for type B samples, values of $S=9.2\times 10^3\ m^{-1}$ and $\xi=0.9996$ are extracted as presented in Figs. 3(c) and 3(d). The parameter S describes the effect of oersted field induced by the applied current as discussed in Eq. (1). In this model, a higher S means a larger angle between the magnetization and the direction of the current. In comparison, the coefficient S for type C sample is three orders of magnitude larger than the type A bilayer sample. This is due to the dipolar field present between the top and the bottom surfaces in $Ni_{81}Fe_{19}$ microstructure which favors opposite magnetization directions in these regions.

The parameter ξ describes any asymmetric effects due to the different current distributions or magnetic properties across the structure. The observation of a second harmonic signal from these type B samples indicates that the parameter ξ is not exactly equal to one. This is interpreted to be the result of a slightly different thickness or slightly different resistance of the top and the bottom Permalloy layers. From our experimental data, the scissoring angle difference between the top and bottom layers for type B samples is about

Downloaded 03 Feb 2010 to 132.163.130.151. Redistribution subject to AIP license or copyright; see http://jap.aip.org/jap/copyright.jsp

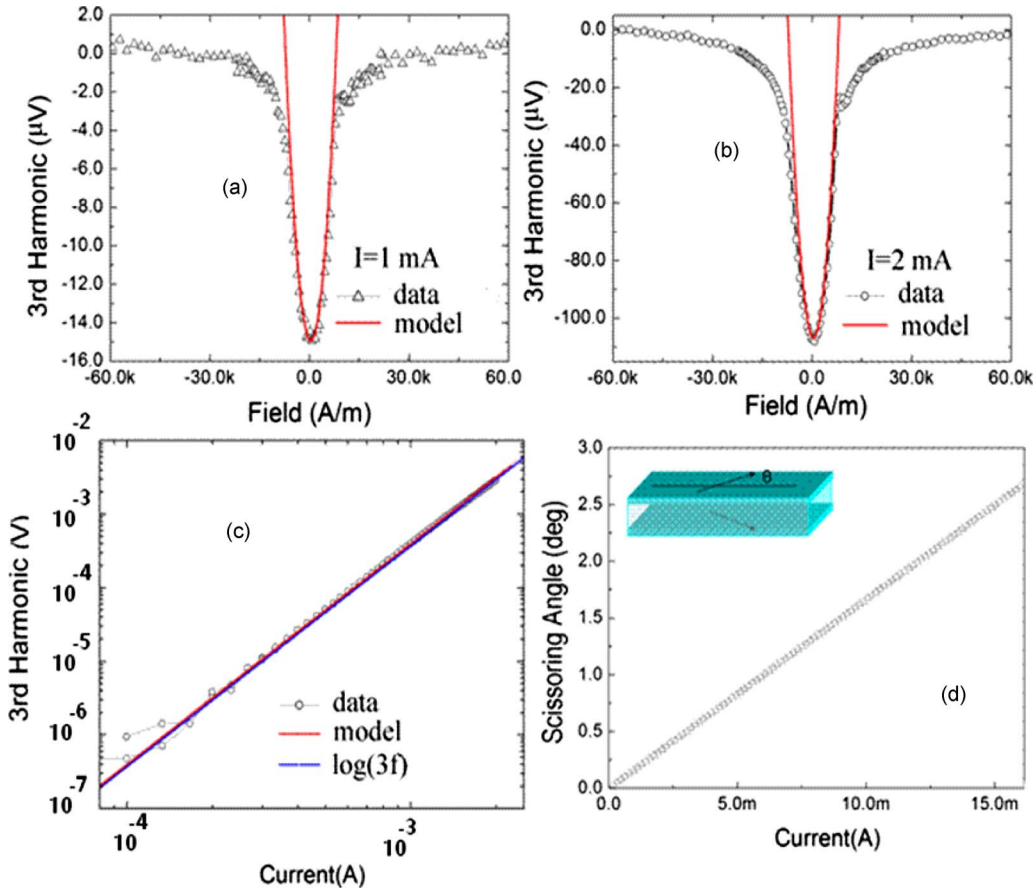

FIG. 4. (Color online) The third harmonic measurement for the single layer $Ni_{81}Fe_{19}$ type C stripe with dimensions of 0.8 μm × 10 nm × 10 μm and current of (a) 1 mA and (b) 2mA, respectively. The current dependence of the third harmonic (c) amplitude change and (d) scissoring angle.

$2.4\times10^{-4\circ}$ at 10 mA total bias current without any external field being present. This is comparable to the rotation angle of type A samples, $4.6\times10^{-4\circ}$, under a similar bias condition. These data indicate that the second harmonic is sensitive to asymmetries in these structures. From our model, if ξ equals to one (as would be expected in a type C sample) then there should be no second harmonic signal.

We use the results of type A bilayer and type B trilayer samples as a reference data to measure the effect on a type C single layer $Ni_{81}Fe_{19}$ microstructure. While no second harmonic signal is evident, the third harmonic is observed to be a parabolic function of the applied field [Figs. 3(e) and 3(f)]. Comparison of this response to the reference data shows that the magnetic scissoring, i.e., the rotation of the magnetization of the outermost magnetic layer of the sample, is in opposite direction and follows the oersted field. The measured data fit well with the magnetic scissoring model and results in a value for $S=7.8\times10^{4}$ m^{-1} as shown in solid line in Figs. 3(e) and 3(f).

Figures 3(f) and 4(a) show that for sample type C with bias current increasing from 400 μA to 1 mA, the third harmonic signal amplitude change increases from 1.5 to 15 μV. A similar behavior is illustrated in Figs. 3(f) and 4(b) in which the current increases from 400 μA to 2 mA and the third harmonic signal amplitude change increases from 1.5 to 110 μV. These comparisons demonstrate that the amplitude of the third harmonic and the model nearly increase with I^3 [shown in Fig. 4(c) by solid line in blue].The scissoring angle of the structure induced by the applied current is calculated from $\theta=\arcsin(SI/H_k)$ in the absence of any external field. Figure 4(d) shows that the measured scissoring angle increases with the bias current. At a current density of 2×10^{8} A/cm^2, a scissoring angle of $\pm2.7°$ is obtained for the type C sample.

Next, we measured the width and the thickness dependence of magnetic scissoring behavior for type C single layer $Ni_{81}Fe_{19}$ and compared the experimental angles to those obtained with OOMMF simulation tool. Samples with thicknesses of 10, 30, and 50 nm and the widths ranging from 0.2 to 1 μm were considered. The effect of the induced oersted field on the magnetic scissoring of these samples was examined by measuring the scissoring angle while keeping the current density the same. Figure 5(a) shows that the sample with a smaller width to thickness ratio has a larger scissoring angle, where angles of up to $\pm20°$ are observed. This indicates that the microstructures with smaller width to thickness ratios demonstrate larger scissoring effect as would be expected from a dipole consideration. The scatter in the data represents the uncertainty in the measurement. Figure 5(b) shows the OOMMF simulation result of a single layer Permalloy microstructure with dimensions of 600 nm × 30 nm × 10 μm at a current density of 2×10^{8} A/cm^2. As shown in Fig. 5(c), the simulated scissoring angle at the center is

Downloaded 03 Feb 2010 to 132.163.130.151. Redistribution subject to AIP license or copyright; see http://jap.aip.org/jap/copyright.jsp

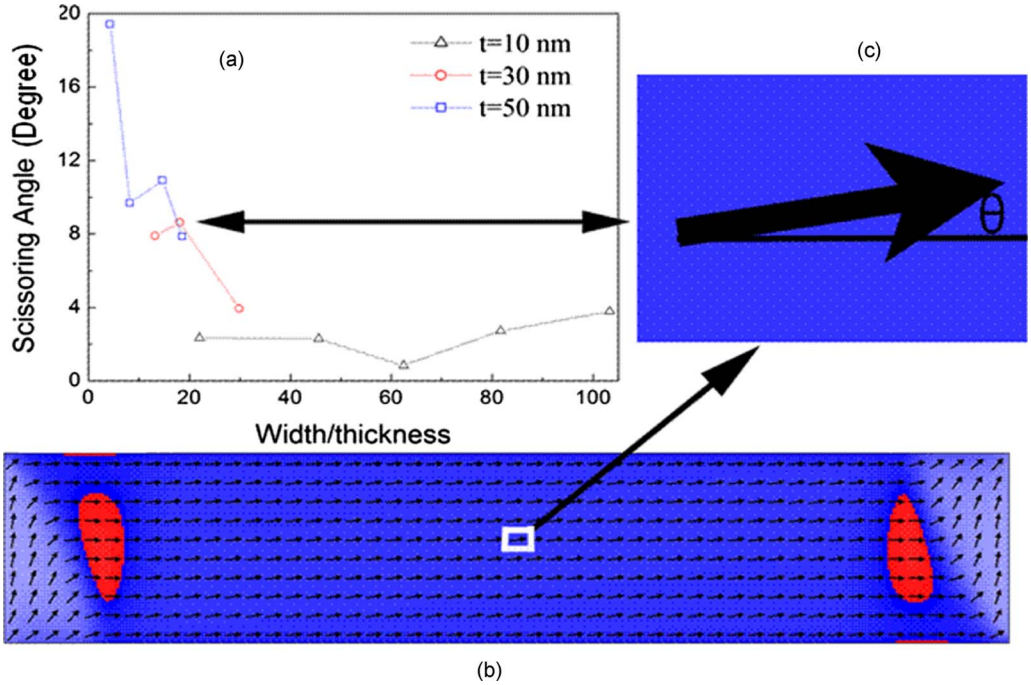

FIG. 5. (Color online) (a) Measurement of the width to thickness ratio dependence of the scissoring angle; the angle is induced by the applied current with the same current density of 2×10^8 A/cm^2. (b) OOMMF simulation for the stripe with dimensions of 0.6 μm$\times$35 nm$\times$2 μm and current density of 2×10^8 A/cm^2. (c) The enlarged picture of the center unit in the simulated stripe, the scissoring angle is 9°.

about ±9° and compares well with the measured experimental angle of ±8.4°.

IV. CONCLUSION

We have investigated and obtained insight into the magnetization behavior in narrow, submicron Permalloy microstructures using the second and third harmonics magneto resistance measurement technique. Both the experimental and simulation results show that a coherent magnetic rotation causes a field-dependent second harmonic and a field-independent third harmonic. Conversely, the magnetic scissoring behavior induces a field-dependent third harmonic signal. We have shown that the magnetic scissoring effect in aluminum/Permalloy microstructures is induced from oersted field generated by applied current. We have observed up to ±20° of magnetic scissoring at a current density of 2×10^8 A/cm^2 for samples with small width to thickness ratios.

ACKNOWLEDGMENTS

This work was supported by the National Institute of Standards and Technology's Competence program.

[1]N. Smith, W. Doyle, D. Markham, and D. LaTourette, IEEE Trans. Magn. **23**, 87 (1987).
[2]J. I. Martin, J. Nogues, K. Liu J. L. Vicent, and I. K. Schuller, J. Magn. Magn. Mater. **256**, 449 (2003).
[3]S. Goolaup, A. O. Adeyeye, N. Singh, and G. Gubbiotti, Phys. Rev. B **75**, 144430 (2007).
[4]M. Steiner, C. Pels, and G. Meier, J. Appl. Phys. **95**, 6759 (2004).
[5]Y. Acremann, J. P. Strachan, V. Chembrolu, S. D. Andrews, T. Tyliszczak, J. A. Katine, M. M. Carey, B. M. Clemens, H. C. Siegmann, and J. Stöhr, Phys. Rev. Lett. **96**, 217202 (2006).
[6]Q. Zhan, W. He, X. Ma, Y. Liang, Z. Kou, N. Di, and Z. Cheng, Appl. Phys. Lett. **85**, 4690 (2004).
[7]L. Berger, J. Appl. Phys. **55**, 1954 (1984).
[8]L. Berger, Phys. Rev. B **33**, 1572 (1986).
[9]L. Thomas, M. Hayashi, X. Jiang, R. Moriya, C. Rettner, and S. S. P. Parkin, Nature (London) **443**, 197 (2006).
[10]M. Yamanouchi, D. Chiba, F. Matsukura, and H. Ohno, Nature (London) **428**, 539 (2004).
[11]F. B. Shelledy and G. W. Brock, IEEE Trans. Magn. **11**, 1206 (1975).
[12]B. A. Everitt, J. Appl. Phys. **87**, 7088 (2000).
[13]A. Aharoni, J. Appl. Phys. **83**, 3432 (1998).
[14]T. Devolder, A. Tulapurkar, Y. Suzuki, C. Chappert, P. Crozat, and K. Yagami, J. Appl. Phys. **98**, 053904 (2005).
[15]M. Carpentieri, G. Finocchio, B. Azzerboni, L. Torres, L. Lopez-Diaz, and E. Martinez, J. Appl. Phys. **97**, 10C713 (2005).
[16]D. Tripathy and A. O. Adeyeye, Phys. Rev. B **79**, 064413 (2009).
[17]OOMMF, NIST object oriented magnetic modeling framework.

Downloaded 03 Feb 2010 to 132.163.130.151. Redistribution subject to AIP license or copyright; see http://jap.aip.org/jap/copyright.jsp